

# Table-top nanodiamond interferometer enabling quantum gravity tests

Marta Vicentini,<sup>1</sup> Ettore Bernardi,<sup>1</sup> Ekaterina Moreva,<sup>1</sup> Fabrizio Piacentini,<sup>1,\*</sup>  
Carmine Napoli,<sup>1</sup> Ivo Pietro Degiovanni,<sup>1</sup> Alessandra Manzin,<sup>1</sup> and Marco Genovese<sup>1</sup>

<sup>1</sup>*INRIM, Strada delle Cacce 91, I-10135 Torino, Italy*

(Dated: June 3, 2024)

Unifying quantum theory and general relativity is the holy grail of contemporary physics. Nonetheless, the lack of experimental evidence driving this process led to a plethora of mathematical models with a substantial impossibility of discriminating among them or even establishing if gravity really needs to be quantized or if, vice versa, quantum mechanics must be “gravitized” at some scale. Recently, it has been proposed that the observation of the generation of entanglement by gravitational interaction, could represent a breakthrough demonstrating the quantum nature of gravity. A few experimental proposals have been advanced in this sense, but the extreme technological requirements (e.g., the need for free-falling gravitationally-interacting masses in a quantum superposition state) make their implementation still far ahead. Here we present a feasibility study for a table-top nanodiamond-based interferometer eventually enabling easier and less resource-demanding quantum gravity tests. With respect to the aforementioned proposals, by relying on quantum superpositions of steady massive (mesoscopic) objects our interferometer may allow exploiting just small-range electromagnetic fields (much easier to implement and control) and, at the same time, the re-utilization of the massive quantum probes exploited, inevitably lost in free-falling interferometric schemes.

## INTRODUCTION

The unification of quantum theory and general relativity has always been one of the key topics in physics, becoming a sort of “holy grail” of contemporary physics thanks to recent technological and theoretical developments. Nonetheless, experimental evidences about this are still missing, allowing for the rise of several different mathematical models [1–3], ranging from string theory [4] to loop gravity [5] and supergravity [6], with a substantial impossibility of discriminating among them or even establishing whether gravity really needs to be quantized or if, vice versa, quantum mechanics must be “gravitized” at some scale. Indeed, even though, so far, quantum theory has proven unchallenged by experimental evidence, there are arguments supporting the idea that quantum mechanics might cease to apply at a certain scale, for instance due to the collapse of macroscopic quantum superpositions [7], with gravity being eventually suggested as the possible cause for this phenomenon [8, 9]. Thus, it is crucial to start an experimental search for quantum gravity effects at small scales [10], e.g. along the line of a recent proposal suggesting that the observation of gravity-induced entanglement could demonstrate (or challenge) the quantum nature of gravity. In particular, Marletto & Vedral [11, 12] and Bose et al. [13] proposed a test of quantum gravitational features, based on the ability of gravity to generate entanglement between two quantum probes – two masses, each in a spatial superposition state.

What exactly this observation would mean has given rise to some debate [10]. Nonetheless, it can be shown, in the framework of constructor theory [14, 15], that it witnesses non-classicality of gravity when one assumes lo-

cality and interoperability of information (i.e. that classical information can be copied) [16]. This experimental scheme has the promising feature that it can probe quantum effects in gravity in a low-energy regime, and below Planck’s scale. Moreover, by the previous considerations, detecting gravitational entanglement would refute a large set of classical theories of gravity in the presence of quantum masses.

Among them, all the semiclassical theories of gravity, as quantum field theory in curved space-time [17], collapse models predicting a collapse at the experiment energy scale [7–9], and other hybrid quantum-classical theories [18, 19]. Detecting entanglement would therefore lead to a major breakthrough, as it would be the first refutation of classical theories of gravity and would confirm that gravity must be quantized – thus achieving the first experimental confirmation of quantum effects in gravity. On the other hand, not detecting entanglement would not demonstrate that gravitational interaction is classical, but would still open several interesting possibilities [10] (e.g., one of the assumptions is wrong, other forces are at play, the magnitude of the effect is too small in a specific quantum gravity theory, etc.).

The challenge, at present, lies in realizing this experiment within available technology [20–33]. Thanks to recent advances in quantum metrology and quantum sensing, one is able to manipulate quantum objects of increasing mass (ranging from nanoparticles to MEMS oscillators), so this task can be deemed to be within reach. Bose et al. proposed to exploit two nanodiamonds (NDs) presenting single nitrogen-vacancy (NV) centers. Both NDs are prepared in a spatially-delocalized quantum superposition by means of a magnetic field gradient [34, 35] acting on the NV-centre spin, and subsequently

they are left subjected only to reciprocal gravitational interaction by letting them fall freely within a vacuum chamber. However, implementing such a free-fall scheme comes with significant technical challenges. It necessitates constructing a magnetic structure that is over 10 meters in size, with features fabricated to a precision of micrometers. Moreover, maintaining such a large structure in high-vacuum and low-temperature conditions is necessary. On top of these challenges, there is the need to develop a large number ( $\gtrsim 10^4$ ) of antennas capable of delivering microwave pulses for achieving quantum control of the spin states of NV centers (or similar color centers [36]), which is essential for performing the DD [37] required to extend the coherence time of the NV centers.

Conversely, here we propose a more straightforward, table-top experimental scheme, capable of creating and manipulating spatially-delocalized ND quantum superpositions and, eventually, achieving the desired gravitational interaction between them in a more practical and better-controlled way. As explained below (see Fig. 1), our proposal involves semi-trapped instead of free-falling NDs, constrained in two directions ( $y$  and  $z$ ) but free to move along the third one ( $x$ ). If gravity presents quantum features, the distance mismatch generated between the spatially-separated superposition components of the two NDs should allow the gravitational potential to entangle them, an impossible task for local operations and classical communication (LOCC) [38, 39]. We will show

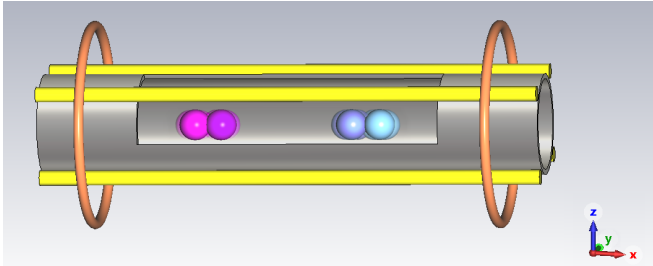


FIG. 1: The proposed experimental scheme is based on two single-NV-centre nanodiamonds (trapped in the  $y$  and  $z$  directions by a gravito-magnetic potential) both in a spatially-delocalized superposition, generated by putting the NV center spin component  $S_x$  in the initial state  $|\psi_S\rangle = \frac{1}{\sqrt{2}}(|-1\rangle + |1\rangle)$  before applying a magnetic field gradient  $B'$  along the  $x$  direction, thus spatially separating the two components of  $|\psi_S\rangle$ . The distance mismatch between the superposition components of the two NDs should allow the gravitational potential to entangle the two NDs, an impossible task for local operations and classical communication (LOCC).

how, besides the much easier implementation, our scheme presents several other advantages compared to the one of Bose and co-workers [13, 34, 35], e.g. the fact that the NDs are not lost after the final measurement and

can be re-initialized for a subsequent run without needing to find and characterize new samples every time, a time-consuming task that would heavily slow down the measurement process.

## SINGLE NANODIAMOND INTERFEROMETER

For simplicity, let us consider the case in which a stationary single-NV-centre ND is left free to move along the  $x$  direction while being constrained in the remaining two ( $y$  and  $z$ ), with the NV-centre spin axis aligned along the unconstrained direction. Such a scenario can be obtained by exploiting a magnetic trap [40–43], with a magnetic field configuration forming a 2D confining potential in the  $y$  and  $z$  directions and leading the dynamics along  $x$ , eventually hosting doughnut-shaped optical tweezers [44] to accurately move the trapped ND in the  $x$ - $y$  plane without destroying it because of excessive heat. After having prepared the single NV-centre of the ND spin component  $S_x$  in the superposition state  $|\psi_S\rangle = \frac{1}{\sqrt{2}}(|-1\rangle + |1\rangle)$  in order to create a spatially-delocalized ND superposition we can generate a magnetic field gradient  $B'$  in the  $x$  direction. The ND Hamiltonian along  $x$  will then read:

$$H_x = \frac{p_x^2}{2m} + \frac{\chi V (B_0 + B'x)^2}{2\mu_0} + \hbar\gamma_e S_x (B_0 + B'x) + \hbar D S_x^2, \quad (1)$$

being, respectively:  $m$ , the ND mass;  $p_x$ , its momentum along  $x$ ;  $V$ , its volume;  $\chi$ , its magnetic susceptibility (assuming for the ND a diamagnetic state);  $\mu_0$ , the vacuum magnetic permeability;  $\gamma_e$ , the gyromagnetic ratio of the electron;  $B_0$ , the bias magnetic field;  $D$ , the zero-field splitting of the NV centre. Classically, the dynamics generated by the Hamiltonian in Eq. (1) would correspond, for two separated particles of opposite spin, to a harmonic oscillation with the same frequency but different equilibrium positions:

$$x_0^{(\pm)}(t) = x_0^{(\pm)}(1 - \cos(\omega t)), \quad (2)$$

being  $x_0^{(\pm)} = -\frac{\chi V B_0 \pm \hbar\gamma_e \mu_0}{\chi V B'}$  the equilibrium position of the particle corresponding to the  $S_x = \pm 1$  spin component, and  $\omega = B' \sqrt{\frac{\chi V}{\mu_0 m}}$  the oscillation frequency.

Conversely, the quantum mechanical version of the Hamiltonian in Eq. (1) reads:

$$\begin{aligned} H_x &= \frac{\hat{p}_x^2}{2m} + \frac{\chi V (B' \hat{\xi})^2}{2\mu_0} + \hbar\gamma_e \hat{S}_x (B' \hat{\xi}) + \hbar D \hat{S}_x^2 \\ &= \hbar\omega \hat{a}^\dagger \hat{a} + \hbar\lambda (\hat{a} + \hat{a}^\dagger) \hat{S}_x + \hbar D \hat{S}_x^2, \end{aligned} \quad (3)$$

with  $\hat{\xi} = \hat{x} + \frac{B_0}{B'}$  and  $\lambda = \gamma_e B' \sqrt{\frac{\hbar}{2m\omega}}$ , corresponding to a shifted harmonic oscillator with ground states:

$$S_x = \pm 1 : \quad \left| \frac{\lambda_{\pm}}{\omega} \right\rangle = e^{-\frac{1}{2} \left| \frac{\lambda_{\pm}}{\omega} \right|^2} \sum_{n=0}^{\infty} \left( \frac{\lambda_{\pm}}{\omega} \right)^n \frac{(a^\dagger)^n}{n!} |0\rangle, \quad (4)$$

being  $\lambda_{\pm} = \lambda_0 \pm \lambda$  and  $\lambda_0 = \frac{B_0}{B'} \sqrt{\frac{m\omega^3}{2\hbar}}$ .

By applying the evolution operator  $\hat{U} = \exp\left(-\frac{i}{\hbar} \int_0^t dt' H_x\right)$  to our ND, initially in the harmonic oscillator ground state  $|0\rangle$ , one obtains:

$$|\alpha(t)\rangle_{\pm} = e^{-i\left(\frac{\omega}{2} - \frac{|\lambda_{\pm}|^2}{\omega}\right)t} \exp\left(\left|\frac{\lambda_{\pm}}{\omega}\right|^2 (1 - e^{-i\omega t})\right) \cdot \left|\frac{\lambda_{\pm}}{\omega} (1 - e^{i\omega t})\right\rangle. \quad (5)$$

In case of  $B_0 \rightarrow 0$ , Eq. (5) describes for the two  $S_x$  components an oscillatory dynamics with equilibrium positions symmetric with respect to the ND rest position (considered as the “0” of the  $x$  axis); the role of the magnetic field  $B_0$  is to shift concurrently the equilibrium position of the harmonic oscillations of both the ND superposition components, as shown in Fig. 2. There, we plot-

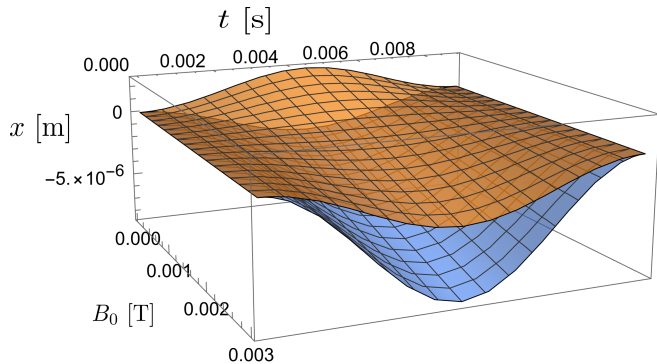


FIG. 2: One-period motion along the  $x$  of the  $S_x = 1$  (orange curve) and  $S_x = -1$  (blue curve) components of a 250 nm diameter ND in a magnetic field gradient  $B' = 10^3$  T/m, as a function of the static magnetic field  $B_0$ . The role of  $B_0$  is to shift of the same amount the equilibrium position of both superposition components.

ted a single oscillation trajectory for both the  $S_x = \pm 1$  components, considering a ND with a 250 nm diameter, a magnetic field gradient (along the  $x$  axis)  $B' = 10^3$  T/m and a magnetic field  $B_0$  varying from 0 to 3 mT. As evident, in the absence of  $B_0$  the two components of the ND superposition follow two symmetric trajectories, while by increasing  $B_0$  the equilibrium positions of both oscillatory motions is shifted of the same amount, leaving the maximum separation between them unperturbed. This can also be appreciated from the ND dynamics in the phase space, reported in Fig. 3. Indeed, Fig. 3a shows the behavior of the  $S_x = \pm 1$  components in the absence of a static magnetic field, when they follow symmetric trajectories. Fig. 3b, instead, highlights how, for  $B_0 = 5 \times 10^{-3}$  T, the shift in the equilibrium positions of the two oscillatory motions starts creating an unbalance in their dynamics. This asymmetry between the two trajectories for non-negligible  $B_0$  values induces a phase

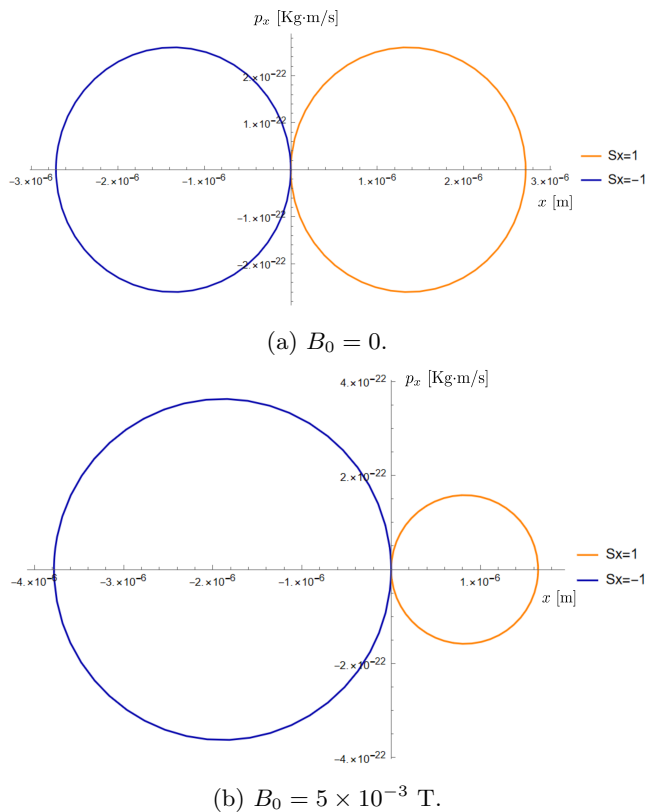


FIG. 3: Phase space diagram of the two ND superposition components, for different values of static magnetic field  $B_0$ .

difference accumulation between the two superposition components  $|\frac{\lambda_{\pm}}{\omega}\rangle$ , that after a whole oscillation will be:

$$\Delta\phi = 4 \frac{\lambda_0 \lambda}{\omega^2} = 2\gamma_e \frac{B_0}{B'} \sqrt{\frac{m\mu_0}{\chi V}}. \quad (6)$$

At time  $t = \frac{2\pi}{\omega}$ , when the two superposition components recombine in the original ND position (i.e.  $x = 0$  in our reference frame), we can measure  $\Delta\phi$  in the NV centre quantum state by means of a Ramsey-like interferometric measurement [45]. By repeating this procedure while varying  $B_0$ , we are able to characterize the generated spatially-delocalized ND superposition, determining if it qualifies for subsequent ND-based quantum gravity experiments.

### Introducing Dynamical Decoupling

As already stressed in previous works [13, 35], the coherence time of NV centres in (nano) diamonds might be not enough to allow performing gravity-related experiments, since the time interval needed for an eventual gravity-induced entanglement between two spatially-delocalized ND superpositions could be  $\sim 1$  s [13], i.e. orders of magnitude above the NV centre coherence times

reported in literature [46–48]. To increase this coherence time one might introduce a dynamical decoupling (DD) mechanism [37], obtained with a train of  $N$  microwave  $\pi$  pulses flipping the sign of the spin component  $S_x$  at a frequency  $\omega_{DD} = N\omega$ . With this kind of mechanism, to keep the Hamiltonian in Eq. (3) time invariant one should flip the direction of the magnetic field vector and its gradient (i.e. change the sign of both  $B_0$  and  $B'$ ) together with the  $S_x$  sign flip needed for the dynamical decoupling. This way, the system dynamics should be the same (except for an eventual bias due to the small but still non-zero flipping time of  $B'$  and  $B_0$ ) as the one given by Eq. (5).

To achieve a locally-confined uniform gradient of the magnetic field, an anti-Helmholtz configuration could be selected for the coil (i.e. a Helmholtz coil with two electromagnets carrying currents with opposite directions) [49]. This way, the necessary flipping of  $B'$  can be easily driven by supplying the coil windings with radiofrequency currents with frequency  $\sim 100$  kHz. If the currents have the same amplitude,  $B_0 \simeq 0$  at the target region center, apart from background noise. Two technical solutions can be adopted to have a non-zero  $x$  component of  $B_0$ : (i) the coil windings are supplied with currents with different amplitude, to produce a dissymmetry in the magnetic field spatial distribution; (ii) the ND is trapped at  $x \neq 0$ , at the cost of reduced uniformity in  $B'$ . This way, to flip simultaneously  $B_0$  and  $B'$  an inversion of the supply currents can be introduced, possibly causing delays to the ND dynamics, which might negatively impact on the DD.

As an alternative, in case a precise enough control of both  $B_0$  and  $B'$  resulted too challenging, one might consider flipping only  $B'$  together with  $S_x$ , leaving  $B_0$  untouched. Given the peculiar form of the Hamiltonian in Eq. (1), this is equivalent to a scenario in which  $B'$  and  $S_x$  are left unperturbed and only  $B_0$  flips, leading to the time-dependent Hamiltonian:

$$\begin{aligned}
 H_x^{(DD)} = & \sum_{i=0}^{\infty} \left( \frac{p_x^2}{2m} + \frac{\chi V (B_0(-1)^i + B'x)^2}{2\mu_0} + \right. \\
 & \left. + \hbar\gamma_e S_x (B_0(-1)^i + B'x) + \hbar D S_x^2 \right) \cdot \\
 & \cdot \left[ \Theta \left( t - \frac{2\pi}{\omega_{DD}} i \right) - \Theta \left( t - \frac{2\pi}{\omega_{DD}} (i+1) \right) \right], \quad (7)
 \end{aligned}$$

being  $\Theta(x)$  the Heaviside theta function. In such a picture, each superposition component of the ND will alternatively swap between two Hamiltonians of the form of Eq. (1),  $H_x^{(\uparrow)}$  and  $H_x^{(\downarrow)}$ , with  $H_x^{(\uparrow\downarrow)} = H_x(\pm B_0)$ . Each of these Hamiltonians is of the form of Eq. (3), both resulting in a (shifted) harmonic oscillator but with different equilibrium positions. Therefore, the global dynamics of the ND wavefunction components can be obtained as a

composition of the dynamics in the single time interval, resulting in a sort of forced oscillatory regime caused by the flipping of the harmonic oscillator equilibrium positions at each DD pulse.

This appears evident when looking at the phase space diagram reported in Fig. 4, obtained considering a static magnetic field  $B_0 = 5 \times 10^{-4}$  T. Indeed, in case of  $N = 4$  (as in Fig. 4a), one can immediately grasp how the trajectory of both superposition components (orange and purple curves for  $S_x = 1$  and  $S_x = -1$ , respectively) initially follows the one dictated by the Hamiltonian in Eq. (3), corresponding to  $H_x^{(\uparrow)}$  in the DD regime (red and blue curves, respectively). Then, in correspondence of the first  $\pi$  pulse, they start to feel a different harmonic potential, and their trajectory becomes a circle centered on the same equilibrium position as the trajectory dictated by the  $H_x^{(\downarrow)}$  Hamiltonian (dashed green and azure curves, respectively). The subsequent  $\pi$  pulse restores  $H_x^{(\uparrow)}$ , hence each ND component makes an arc centered on its initial equilibrium position until the following pulse, that makes both  $S_x$  components follow the trajectory stemming from  $H_x^{(\downarrow)}$  to return to their initial position.

For increasing  $\omega_{DD}$ , e.g. for  $N = 20$  as in Fig. 4b, the frequent flipping between the two Hamiltonians starts to highlight some “gearwheel” dynamics, that seems to approach the one of a harmonic oscillator with an average equilibrium position between the ones given by  $H_x^{(\downarrow)}$  and  $H_x^{(\uparrow)}$ . This is confirmed by the asymptotic behavior obtained for  $\omega_{DD} \gg \omega$  (i.e., for the scenario of an actual DD implementation), as shown in Fig. 4c.

Remarkably, one could notice how, even though the non-negligible  $B_0$  considered here already produces a phase difference between the two ND superposition components without DD (or for a  $B_0$  sign flipping accordingly with  $\omega_{DD}$ ), the trajectories dictated by  $H_x^{(DD)}$  are symmetric with respect to the origin, as it was before for  $B_0 = 0$  (see Fig. 3b). This means that, on the one hand, when implementing DD one needs to flip both  $B_0$  and  $B'$  together with the DD pulses to observe some  $B_0$ -induced phase difference between the two ND superposition components. On the other hand, the fact that DD makes our system insensitive to  $B_0$  means that our ND superposition is unperturbed by residual static force fields potentially present in our setup (in this case, to characterize the ND superposition one could initialize the NV-centre  $S_x$  state in one of the  $|\psi_{0\pm}\rangle = \frac{1}{\sqrt{2}}(|0\rangle \pm |1\rangle)$  states instead of  $|\psi_S\rangle$ ).

Once we achieve a fully-controllable spatially-superposed ND, by trapping two of them at once we are able to experimentally investigate potential quantum traits in gravity.

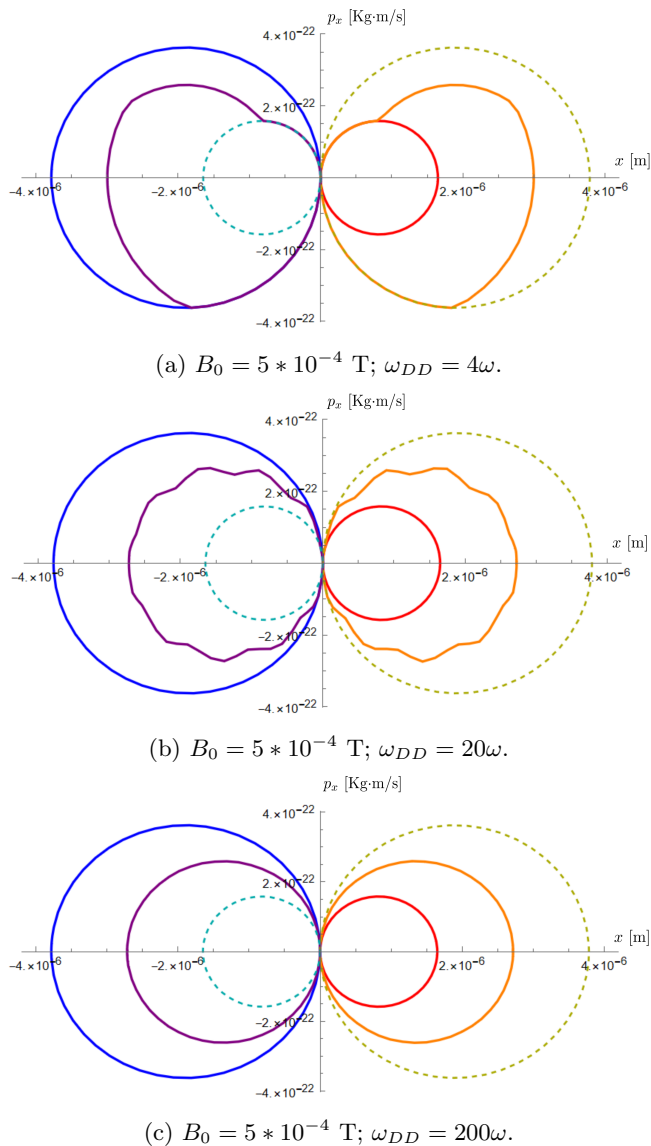


FIG. 4: Plots (a-c): Phase space diagram ( $X$ - and  $Y$ -axis, respectively: position and momentum along the  $x$  direction, expressed in SI units) of the two ND superposition components, for different  $\omega_{DD}$  values. Red curve: dynamics generated by  $H_x^{(\uparrow)}$  for  $S_x = 1$ . Green dashed curve: dynamics generated by  $H_x^{(\downarrow)}$  for  $S_x = 1$ . Orange curve: dynamics generated by  $H_x^{(DD)}$  for  $S_x = 1$ . Blue, azure-dashed and purple curves, respectively: dynamics generated by  $H_x^{(\uparrow)}$ ,  $H_x^{(\downarrow)}$  and  $H_x^{(DD)}$  for the  $S_x = -1$  superposition component.

### TABLE-TOP QUANTUM GRAVITY EXPERIMENT

The main difference between our proposal and other ones [11–13] is that we aim to exploit (partially) confined massive superpositions instead of free-falling ones.

Specifically, we need two spatially-delocalized ND superpositions confined at once in the same trap, as in Fig. 1. For this purpose, single-NV-centres with high (DD-enhanced) coherence time will be fabricated and characterized by means of single-photon Hanbury-Brown & Twiss interferometry [50] and optically-detected magnetic resonance.

Selected NDs will be ejected from the growth array via a blister-based laser-induced forward transfer (LIFT) technique [51], essentially pushing the ND from the donor (the array) to the acceptor (the trap). The magnetic trap will confine the two NDs in the  $z$  and  $y$  directions by means of a 2D magnetic potential, while the position of each ND in the (unconstrained)  $x$  direction can be controlled, e.g., with doughnut-shaped optical tweezers, to reduce the light absorption by the trapped NDs, which causes thermal damage in vacuum [52].

As an alternative to the meters long permanent magnet configuration needed for the ND free fall [35], in our configuration one can exploit a time-varying magnetic field having a spatially-uniform gradient generated with an anti-Helmholtz coil [49]. Furthermore, in our case the DD can be implemented by a single microwave antenna instead of the  $\gtrsim 10^4$  antennas needed in a free-fall experiment, requiring the construction of meters long magnets with micro-structures of the order of the  $\mu\text{m}$ .

In refs. [12, 13] it was shown that, despite the weakness of gravity, eventual quantum features in the gravitational interaction between two ND spatial superpositions in adjacent matter-wave interferometers can entangle the NDs (an effect that cannot be achieved by local operations and classical communication [53]). After characterizing the ND spatial superpositions with the methodology described in the previous section, the quantum gravity experiment will be run following the steps reported in Fig. 5. For this purpose, we should try to avoid unwanted interactions that, being stronger than gravity, would shield its effect. The first effect that we will consider is the static [13] and dynamical [54] Casimir-Polder interaction [13, 54–56] bounding the minimum distance between the two NDs, with a first estimate to 200  $\mu\text{m}$  to keep such effect one order of magnitude below the gravitational interaction [13]. We assume a scenario in which two NDs are situated in the same diamagnetic trap at a distance  $d \sim 300\text{--}400 \mu\text{m}$  along the  $x$  direction, at low internal temperature (4 K) and low pressure (both conditions are required for suppressing decoherence), see Fig. 5a. Then, we prepare the spatial superposition of their spins by applying  $B'$  in order to achieve the maximally-separated spatial superposition for each ND (Fig. 5b). Afterwards,  $B'$  is turned off, and only gravitational interaction between the ND superpositions remains. The duration of this step should be adequately chosen to achieve significant entanglement between the two NDs (see Fig. 5c). Then, the spatial superposition of each ND should be recombined along  $x$  by restoring  $B'$  (see Fig. 5d). Finally,

a single-shot measurement of the global spin state of two NDs is performed at the end of the process, to detect the eventual presence of gravitationally-induced entanglement between them (see Fig. 5e).

This configuration presents several advantages with respect to the free-falling ones. For example, it will allow switching from a meters long micro-featured structure to a more compact table-top setup, with a much easier low-temperature and vacuum management. Such a setup also grants a vastly more versatile and controllable DD implementation, granting much better results in terms of NV-centres coherence time extension. Furthermore, after the final measurement on their NV centres, we do not lose the NDs (as happens, instead, in a free-fall scheme), allowing us to recycle them for another experimental run without the need of finding and characterizing new samples for each run, a time-consuming task that would heavily slow down the experiment. Finally, the re-use of the same NDs for the whole experiment intrinsically allows avoiding “noise” contributions arising from fabrication discrepancies among the different NDs needed in schemes where new samples are needed in each experimental run.

## CONCLUSIONS

The eventual observation of the generation of entanglement due to gravitational interaction between two nanomasses both in a spatially-delocalized superpositions [11–13] (or the non-generation of it) would represent a breakthrough in physics, since it would become a first hint of the (non) quantum nature of gravitational interactions [57] as well as the cornerstone of experimental quantum gravity studies [10].

Since such an extremely challenging experiment relies on optimal and precise control of quantum superpositions of massive objects, in this paper we propose and analyse in detail the possibility of realising a table-top setup for producing, controlling and testing spatial superpositions of single-NV-centre NDs. We illustrate the ND superposition components behavior in different scenarios, showing how the implementation of a DD mechanism, besides extending the NV-centre coherence time, could make our quantum superposition robust against potential biases induced by stationary fields. By adding a second spatially-delocalized ND to the magnetic trap and regulating the distance between the two NDs by means of properly-shaped optical tweezers, our system could allow for a table-top experiment aiming at pinpointing (eventual) quantum features in the gravitational interaction by observing gravity-induced entanglement (impossible to stir by local operations and classical communication) between the two NDs. Furthermore, our configuration features many advantages with respect to other proposals in literature [12, 13, 57], e.g. the fact of being realisable with present technologies without extreme technical

requests (as for a free-falling experiment) or the possibility of keeping the NDs after each measurement, allowing their re-use in subsequent runs without needing to find (and trap) new ND samples run by run.

Finally, it is worth mentioning that, being sensitive to extremely weak external fields, this kind of interferometers would also qualify as an innovative and very powerful quantum sensor.

## ACKNOWLEDGMENTS

This work was financially supported by the project QuaFuPhy (call “Trapezio” of Fondazione San Paolo), by the Qu-Test project, which has received funding from the European Union’s Horizon Europe Research and Innovation Programme under grant agreement No. 101113901, and by the project 23NRM04 NoQTeS. The project 23NRM04 NoQTeS has received funding from the European Partnership on Metrology, co-financed from the European Union’s Horizon Europe Research and Innovation Programme and by the Participating States. This work was also funded by the MUR project AQuTE, grant No. 2022RATBS4 (call PRIN 2022). We thank Chiara Marletto and Vlatko Vedral for fruitful discussions.

---

\* f.piacentini@inrim.it

- [1] C. Kiefer, *ISRN Math. Phys.* 2013, 509316 (2013).
- [2] C. Rovelli, *gr-qc*0006061 (2001)
- [3] V. Vedral, *arXiv*:2204.01718 (2022).
- [4] A. Sagnotti & A. Sevrini, *Riv. Nuov. Cim.* 31, 423 (2008).
- [5] C. Rovelli, *Living Rev. Rel.* 1, 1 (1998).
- [6] L. Castellani, *arXiv*:2211.04318, in *Handbook of Quantum Gravity* (2023).
- [7] A. Bassi & G. C. Ghirardi, *Phys. Rept.* 379, 257 (2003).
- [8] L. Djosi, *J. Phys.: Conf. Ser.* 174, 012002 (2009).
- [9] R. Penrose, *Found. Phys.* 44, 557 (2014).
- [10] A. Addazi et al., *Progr. in Part. and Nucl. Phys.* 125, 103948 (2022).
- [11] C. Marletto & V. Vedral, *Nature* 547, 156 (2017)
- [12] C. Marletto & V. Vedral, *Phys. Rev. Lett.* 119, 240402 (2017).
- [13] S. Bose et al., *Phys. Rev. Lett.* 119, 240401 (2017).
- [14] D. Deutsch, C. Marletto, *Proc. R. Soc. A* 471, 2174 (2014).
- [15] C. Marletto et al., *Phys. Rev. Lett.* 128, 080401 (2022).
- [16] C. Marletto and V. Vedral, *Phys. Rev. D*, 102, 086012 (2020).
- [17] N. Birrel & P. C. Davies, “Quantum field theory in curved spacetime”, CUP, 1982.
- [18] C. Barcelo et al., *Phys. Rev. A* 86, 042120 (2012).
- [19] T. N. Sherry & E. C. G. Sudarshan, *Phys. Rev. D* 18, 4580 (1978).
- [20] S. Rijavec, M. Carlesso, A. Bassi, V. Vedral, and C. Marletto, *New J. Phys.* 23, 043040 (2021).

- [21] R. Howl et al., PRX Quantum 2, 010325 (2021).
- [22] Y. Margalit et al. Sci. Adv. 7, eabg2879(2021).
- [23] C. Henkel & R. Folman, AVS Quant. Sci. 4, 025602 (2022).
- [24] R. J. Marshman, A. Mazumdar, R. Folman, and S. Bose, Phys. Rev. Res. 4, 023087 (2022).
- [25] Y. Japha & R. Folman, arXiv:2202.10535 (2022).
- [26] C. Henkel & R. Folman, arXiv:2305.15230 (2023).
- [27] F. Hanif et al., arXiv:2307.08133 (2023).
- [28] L. Braccini, M. Schut, A. Serafini, A. Mazumdar, and S. Bose, arXiv:2312.05170 (2023).
- [29] T. Feng, C. Marletto, and V. Vedral, arXiv:2311.08971 (2023).
- [30] M. Toroš, M. Schut, P. Andriolo, S. Bose, and A. Mazumdar, arXiv:2405.04661 (2024).
- [31] MZ. Wu, M. Toroš, S. Bose, and A. Mazumdar, arXiv:2404.15455 (2024).
- [32] Q. Xiang, R. Zhou, S. Bose, and A. Mazumdar, arXiv:2404.04210 (2024).
- [33] R. J. Marshman, S. Bose, A. Geraci, and A. Mazumdar, Phys. Rev. Lett. 109, 030401 (2024).
- [34] C. Wan et al., Phys. Rev. Lett. 117, 143003 (2016).
- [35] B. D. Wood et al., Phys. Rev. A 105, 012824 (2022).
- [36] D. Gatto Monticone et al., New J. of Phys. 16, 053005 (2014).
- [37] J. S. Pedernales, G. W. Morley, and M. B. Plenio, Phys. Rev. Lett. 125, 023602 (2020).
- [38] C. Bennett, D. DiVincenzo, J. Smolin & W. Wootters, Mixed-state entanglement and quantum error correction. Phys. Rev. A 54, 3824 (1996).
- [39] R. Horodecki, P. Horodecki, M. Horodecki & K. Horodecki, Rev. Mod. Phys. 81, 865 (2009).
- [40] D. E. Pritchard, Phys. Rev. Lett. 51, 1336 (1983).
- [41] P. Treutlein, P. Hommelhoff, T. W. Hansch, and J. Reichel, Phys. Rev. Lett. 93, 219904 (2004).
- [42] J. Fortágh & C. Zimmermann, Rev. Mod. Phys. 79, 235 (2007).
- [43] L. Baum et al., Phys. Rev. Lett. 124, 133201 (2020).
- [44] M. Geiselmann et al., Nat. Nanotech. 8, 175 (2013).
- [45] L. M. K. Vandersypen & I. L. Chuang, Rev. Mod. Phys. 76, 1037 (2004).
- [46] N. Bar-Gill, L. M. Pham, A. Jarmola, D. Budker, and R. L. Walsworth, Nat. Commun. 4, 1743 (2013).
- [47] E. Bernardi, R. Nelz, S. Sonusen, and E. Neu, Crystals 7, 124 (2017).
- [48] B. D. Wood et al., Phys. Rev. B 105, 205401 (2022).
- [49] P. Jansen & F. Merkt, Progr. In Nucl. Magn. Res. Spectr. 102-121, 118-148 (2020)
- [50] D. Gatto Monticone et al., Phys. Rev. Lett. 113, 143602 (2014).
- [51] M. S. Komlenok et al., Phys. Status Solidi A 218, 2000269 (2020).
- [52] L.-M. Zhou et al., Laser Phot. Rev. 11, 1600284 (2017).
- [53] R. J. Marshman, A. Mazumdar, and S. Bose, Phys. Rev. A 101, 052110 (2020).
- [54] P. Barcellona et al., Phys. Rev. A 93, 032508 (2016).
- [55] T. W. van de Kamp, R. J. Marshman, S. Bose, and A. Mazumdar, Phys. Rev. A 102, 062807 (2020).
- [56] G. Amit et al., Phys. Rev. Res. 5, 013150 (2023).
- [57] C. Marletto and V. Vedral, under review for Rev. Mod. Phys.

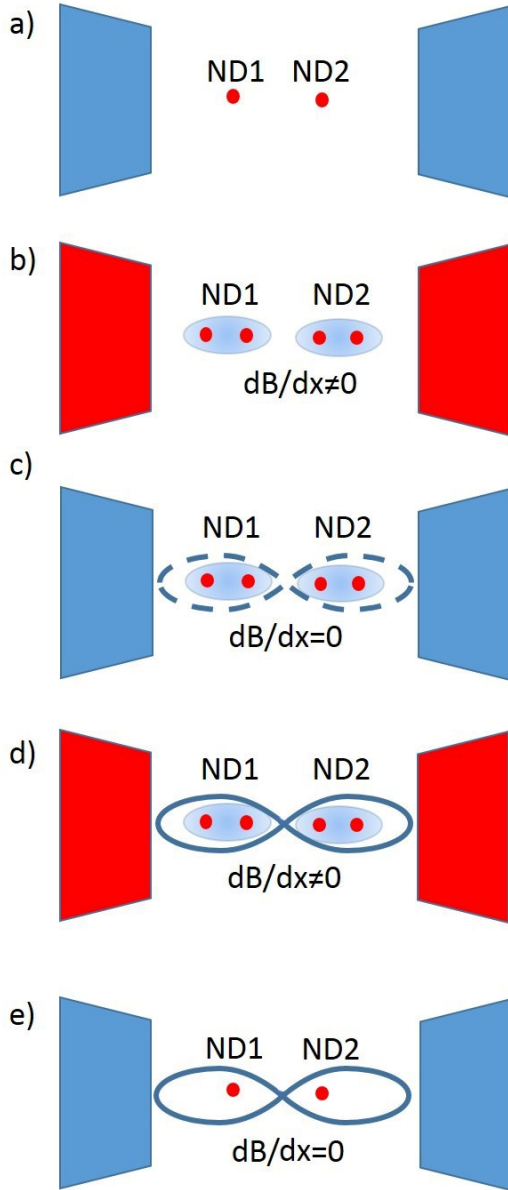


FIG. 5: Step-by-step pictorial scheme of the experiment addressed to unveiling the quantum features of gravity with adjacent ND superpositions: a) two single-NV-centre NDs are confined in the same trap along the  $y$  and  $z$  positions, leaving  $x$  unconstrained; b) a magnetic gradient  $B' = dB/dx$  is generated, allowing to put both NDs in a spatially-delocalized superposition; c)  $B'$  is switched off, to leave the two superpositions freely-evolving by gravitational interaction; d)  $B'$  is turned on again, to recombine each of the two spatial superpositions; e)  $B'$  is turned off again, and a correlated measurement of the two NV-centres is performed, to detect the eventual presence of entanglement between them.